Realization of ultralow power phase locking by optimizing *Q* factor of resonant photodetector

Jin-Rong Wang(王锦荣), Hong-Yu Zhang(张宏宇), Zi-Lin Zhao(赵子琳), and Yao-Hui Zheng(郑耀辉)

Citation: Chin. Phys. B, 2020, 29 (**12**): 124207. DOI: 10.1088/1674-1056/abbbfb
Journal homepage: http://cpb.iphy.ac.cn; http://iopscience.iop.org/cpb

What follows is a list of articles you may be interested in

Realization of ultralow power phase locking by optimizing *Q* factor of resonant photodetector

Jin-Rong Wang(王锦荣), Hong-Yu Zhang(张宏宇), Zi-Lin Zhao(赵子琳), and Yao-Hui Zheng(郑耀辉)
Chin. Phys. B, 2020, 29 (**12**): 124207. DOI: 10.1088/1674-1056/abbbfb

High efficiency sub-nanosecond electro-optical *Q*-switched laser operating at kilohertz repetition frequency

Xin Zhao(赵鑫), Zheng Song(宋政), Yuan-Ji Li(李渊骥), Jin-Xia Feng(冯晋霞), Kuan-Shou Zhang(张宽收)
Chin. Phys. B, 2020, 29 (**8**): 084205. DOI: 10.1088/1674-1056/ab8ac4

Optical nonreciprocity in a piezo-optomechanical system

Yu-Ming Xiao(肖玉铭), Jun-Hao Liu(刘军浩), Qin Wu(吴琴), Ya-Fei Yu(於亚飞), Zhi-Ming Zhang(张智明)
Chin. Phys. B, 2020, 29 (**7**): 074204. DOI: 10.1088/1674-1056/ab8abf

A low-noise, high-SNR balanced homodyne detector for the bright squeezed state measurement in 1-100 kHz range

Jin-Rong Wang(王锦荣), Qing-Wei Wang(王庆伟), Long Tian(田龙), Jing Su(苏静), Yao-Hui Zheng(郑耀辉)
Chin. Phys. B, 2020, 29 (**3**): 034205. DOI: 10.1088/1674-1056/ab683b

Optical enhanced interferometry with two-mode squeezed twin-Fock states and parity detection

Li-Li Hou(侯丽丽), Shuai Wang(王帅), Xue-Fen Xu(许雪芬)
Chin. Phys. B, 2020, 29 (**3**): 034203. DOI: 10.1088/1674-1056/ab6837

RAPID COMMUNICATION

Realization of ultralow power phase locking by optimizing Q factor of resonant photodetector*

Jin-Rong Wang(王锦荣)[1], Hong-Yu Zhang(张宏宇)[1,2], Zi-Lin Zhao(赵子琳)[1,2], and Yao-Hui Zheng(郑耀辉)[1,3,†]

[1] *State Key Laboratory of Quantum Optics and Quantum Optics Devices, Institute of Opto-Electronics, Shanxi University, Taiyuan* 030006, *China*
[2] *Department of Electronics and Information Technology, Shanxi University, Taiyuan* 030006, *China*
[3] *Collaborative Innovation Center of Extreme Optics, Shanxi University, Taiyuan* 030006, *China*

(Received 31 July 2020; revised manuscript received 21 August 2020; accepted manuscript online 28 September 2020)

We design and construct a resonant photodetector (RPD) with a Q factor of 320.83 at the resonant frequency of 38.5 MHz on the basis of a theoretical analysis. Compared with the existing RPD under the same conditions, the signal-to-noise-ratio of the error signal is increased by 15 dB and the minimum operation power is reduced from −55 dBm to −70 dBm. By comparing the standard deviations of the stability curves, we confirm that the RPD has a dramatic improvement on ultralow power extraction. In virtue of the RPD, we have completed the demonstration of channel multiplexing quantum communication.

Keywords: quantum optics, photodetector, Q factor

PACS: 42.50.−p, 85.60.Gz **DOI:** 10.1088/1674-1056/abbbfb

1. Introduction

Pound–Drever–Hall (PDH) technique, as a powerful and elegant locking method, has been widely adopted to achieve a narrow-linewidth and low-noise laser by stabilizing the frequency of the laser to a high-finesse optical cavity.[1–6] Precision metrology,[7–11] atomic[12,13] and molecular[14–16] manipulations have directly benefited from the resulting improvement in laser stability. For example, interferometric measurements such as the search for gravitational waves critically depend on the availability of narrow-linewidth laser systems with extremely low frequency and amplitude noise.[7,8] Atomic clocks based on optical transitions also require extremely stable laser sources to accurately probe the sub-Hertz linewidths available in laser-cooled samples.[12] Also, the generation of the squeezed state of light[17–23] requires several PDH feedback loops to stably lock the cavity length and the relative phase. Under the motivation of gravitational wave detectors, the squeezing strength is gradually increased, reaching the maximum value of 15 dB at 1064 nm.[24–26] It is worthy of noting that the setup with the squeezing factor of 15 dB is not actively stabilized. However, the error signal extraction for active stabilization will introduce the inevitable loss that reduces the squeezing factor. The narrow-band detected signal simplifies the design of the photodetector, whose high Q factor will promote the explosive increase of the gain and realize the error signal extraction with negligible loss. It is important for implementing a high-quality PDH feedback loop without notably degrading the squeezing factor.

The cavity length locking and the relative phase locking between two beams can be realized by utilizing the PDH technique with the same feedback loops, although the references are different.[27] As the first stage of the feedback loop, it is vital to design a high signal-to-noise ratio (SNR) photodetector. In virtue of the design idea of the resonant receiver, we obtained a high gain resonant photodetector (RPD) with a Q factor of 97.6 at the frequency of 58.6 MHz by utilizing a LC circuit to couple the photodiode to the load resistance directly.[28] Subsequently, by adding a winding transformer between the photodiode and the load resistance, the Q factor of the RPD was close to 100 in the frequency region of higher than 100 MHz.[29] Except for the extension of the resonant frequency, the improvement of the Q factor is another eternal pursuit of the RPD.

In this paper, we design and construct a RPD with a Q factor of 320.83 at the resonant frequency of 38.5 MHz on the basis of a theoretical analysis. Under the same conditions, the SNR of the error signal of the new-designed RPD is about 15 dB higher than that of the existing RPD. In virtue of the RPD, we demonstrate an actively relative phase stabilization of signal power of −70 dBm with a local beam of 0 dBm, which has a standard deviation of 264.69 mrad. The high-Q RPD effectively reduces the loss of the error signal extraction. In the case of bright squeezed light of 15 dB with the power of 10 μW, the extraction loss decreases from 1% to 0.17% and the squeezing factor increases from 13.84 dB to 14.78 dB.

*Project supported by the National Natural Science Foundation of China (Grant Nos. 62027821, 11654002, 11874250, and 11804207), the National Key R&D Program of China (Grant No. 2016YFA0301401), the Key R&D Program of Shanxi, China (Grant No. 201903D111001), the Program for Sanjin Scholar of Shanxi Province, the Program for Outstanding Innovative Teams of Higher Learning Institutions of Shanxi, China, and the Fund for Shanxi "1331 Project" Key Subjects Construction, China.

†Corresponding author. E-mail: yhzheng@sxu.edu.cn

2. Photodetector design

As the first stage of the feedback loop, it is vital to design a high SNR photodetector. In the PDH technique, the SNR of the feedback loop is mainly determined by that of the photodetector. Compared with the conventional broad-band photodetector, the RPD can not only significantly boost the signal at the resonant frequency, but also effectively suppress a large amount of noise outside the bandwidth, which represents a well-established technique for extracting the high-SNR error signal.[28] The performance of the RPD is often evaluated by the Q factor. As the Q factor increases, the 3-dB bandwidth of the RPD is reduced and the overall response is increased, hence the SNR of the error signal is improved.

2.1. Theoretical analysis of the Q factor

The detailed circuit schematic of the RPD has been demonstrated.[28] Figure 1(a) shows a circuit layout of the RPD based on the parallel LC resonant circuit, which is composed of the junction capacitance C of the photodiode and an inductor. And its equivalent circuit is displayed in Fig. 1(b). The shunt resistance of the photodiode can be neglected compared to the impedance at the resonant frequency. The resonant frequency and the impedance at the resonant frequency are expressed by[28,30]

$$f_{\rm res} = \frac{w_{\rm res}}{2\pi} = \sqrt{\frac{1}{LC} - \frac{R_{\rm loss}^2}{L^2}}, \tag{1}$$

$$Z(w_{\rm res}) = R_{\rm res} = \frac{L}{R_{\rm loss}C}. \tag{2}$$

In the narrowband approximation, the frequency-dependent impedance of the parallel resonant circuit is a first-order band-pass response around $w_{\rm res}$, characterized by the cutoff frequency (i.e., the bandwidth) of

$$f_{\rm c} = \frac{1}{2\pi}\frac{1}{2(R_{\rm res} - R_{\rm loss})C}. \tag{3}$$

The Q factor is given by the ratio of the resonant frequency to the 3-dB bandwidth, reading

$$Q = \frac{f_{\rm res}}{2f_{\rm c}} = \left(\frac{L}{R_{\rm loss}C} - R_{\rm loss}\right)\sqrt{\frac{C}{L} - \left(\frac{R_{\rm loss}C}{L}\right)^2}. \tag{4}$$

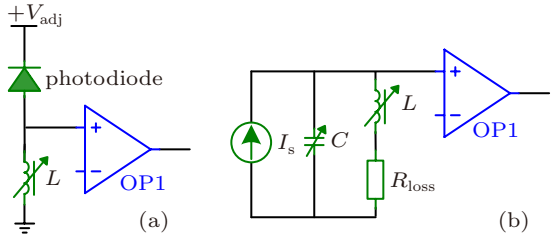

Fig. 1. Circuit layout of the RPD based on the parallel LC resonant circuit (a) and its equivalent circuit (b). All losses of the resonant circuit are modelled by the resistance $R_{\rm loss}$. The junction capacitance C of the photodiode varies with the bias voltage applied on it.

Usually $R_{\rm loss}$ is much smaller than $R_{\rm res}$ and can be ignored, leading to $Q = \sqrt{L/C}/R_{\rm loss}$ and $R_{\rm res} = Q^2 R_{\rm loss}$. The peak impedance increases linearly with the square of the Q factor, and the optical power required for the error signal extraction is reduced. In order to optimize the phase stabilization performance for ultralow power, we expect the Q factor and peak impedance to be as large as possible. The high Q factor can be achieved by minimizing the junction capacitance C that depends on the reverse-bias voltage. However, the junction capacitance C is restricted to a limited range due to the power dissipation and reverse breakdown voltage of the photodiode. As the inductance L is increased, the Q factor is improved according to the above expression. But the winding resistance of the inductor also increases with the inductance. As a part of total loss resistance $R_{\rm loss}$, the winding resistance has an adverse effect on the Q factor. Therefore, there is a trade-off between the inductance L and Q factor. Due to the high-frequency skin effect and parasitic capacitance of the inductor, it is impossible to accurately evaluate the total loss resistance $R_{\rm loss}$ at the high frequency, the Q factor can be only optimized by an experimental procedure.

2.2. Implementation of the high Q factor

The gain and Q factor of the RPD can be characterized by its transfer function in the frequency domain. The measured setup has been demonstrated in more details in Ref. [28].

The detailed regulation procedure is shown below. Firstly, we choose an appropriate combination of the inductor and photodiode (junction capacitance) on the basis of the required resonant frequency. Secondly, the inductor with small winding resistance is handpicked according to the direct current (DC) resistance of the inductor. At last, we finely regulate the inductance by changing the magnetic core position, aiming to reach the required resonant frequency. The success of the regulation process is confirmed at the network analyzer by monitoring the Q factor at the resonant frequency to reach the maximum.

According to the regulation method described above, we measure the transfer functions of the new-designed and existing RPDs and the results are shown in Fig. 2. The resonant frequency is 38.5 MHz and the 3-dB bandwidths of the new-designed and existing RPDs are 0.12 MHz and 0.29 MHz, respectively. The Q factor of the new-designed RPD is 320.83 that is calculated from the measured result. Further increase in Q factor is mainly limited by the winding resistance of the inductor. The Q factor of the new-designed RPD is approximately 2.5 times of that of the existing RPD, corresponding to 6 times of increase in gain at the resonant frequency. The high gain allows us to obtain a stable phase locking with a weak power. For the case of bright squeezed light of 15 dB with the power of 10 μW, the extraction loss decreases from 1% to 0.17% and the squeezing factor increases from 13.84 dB to 14.78 dB. This provides an important technology for quantum optics experiments.[28,29]

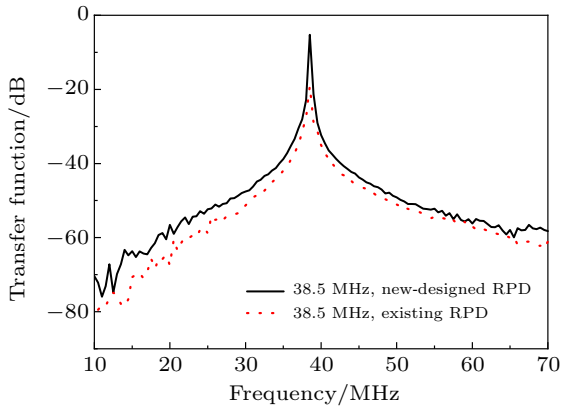

Fig. 2. The transfer functions of the new-designed and existing RPDs.

3. Experimental results and analysis

To evaluate the improvement of the new-designed RPD on the PDH technique, we construct a relative phase stabilization setup between a local beam and a weak beam, shown in Fig. 3. The laser source is a home-made single-frequency Nd:YVO4 laser at 1064 nm and its output power can be conveniently adjusted by a half-wave plate (HWP1) and a polarization beam splitter (PBS1). The most important optical component is a beam splitter consisting of a HWP2 and a PBS2, which can be employed to finely tune the splitting ratio. The linearly s-polarized beam incident on the electro-optic modulator (EOM) is ensured by using the HWP3. The reflected beam from the PBS2, whose power can be adjusted by the optical attenuation plate (OAP), interferes with a local beam on a 50/50 beamsplitter, which is used to simulate the detection of a squeezed state. One of the outputs is directly fed into the RPD to extract an error signal. The output of the RPD is demodulated, and then fed back to the piezoelectric transducer (PZT) through the proportion integration differentiation (PID) calculation and the high voltage (HV) amplification. The other is sensed by a specially-designed photodetector (PD) connected with an oscilloscope (OSC) to indirectly deduce the power of the weak beam. A radio-frequency signal from the signal generator (SG) is split into two parts: one is used to drive the EOM and the other serves as the electronic local oscillator to demodulate the RPD's output.

When the modulation depth is 0.1 and the power of the local beam is 0 dBm, the existing and new-designed RPDs are tested at a weak power of −40 dBm respectively. The results are shown in Fig. 4. Compared to the existing RPD, the SNR improvement with the new-designed RPD is rather obvious. The amplitude with the new-designed RPD is amplified by approximately 6 fold in Fig. 4. Here, the SNR is defined as the ratio of the peak–peak value of the error signal (V_{pp} in Fig. 4)

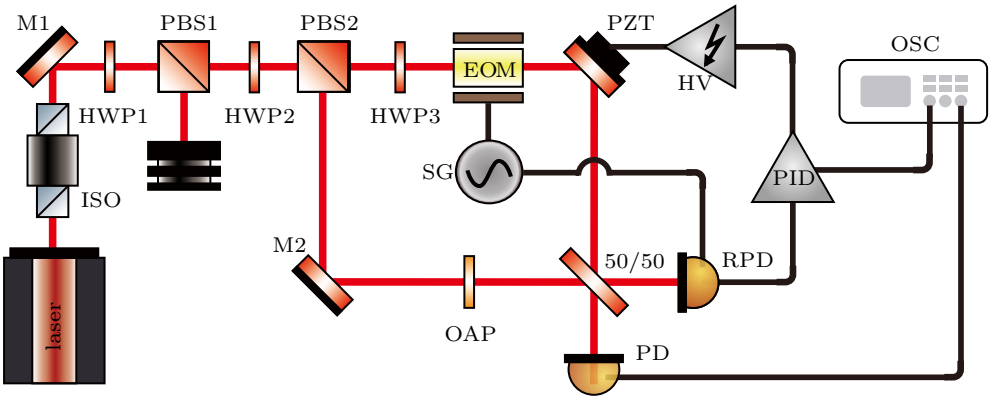

Fig. 3. Experimental setup for measuring the locking stability of the servo-control system for the phase-locking between a local beam and a weak beam. ISO: isolator; HWP: half-wave plate; PBS: polarization beam splitter; EOM: electro-optic modulator; SG: signal generator; PZT: piezoelectric transducer; OAP: optical attenuation plate; RPD: resonant photodetector; PD: photodetector; PID: proportion integration differentiation; HV: high voltage; OSC: oscilloscope.

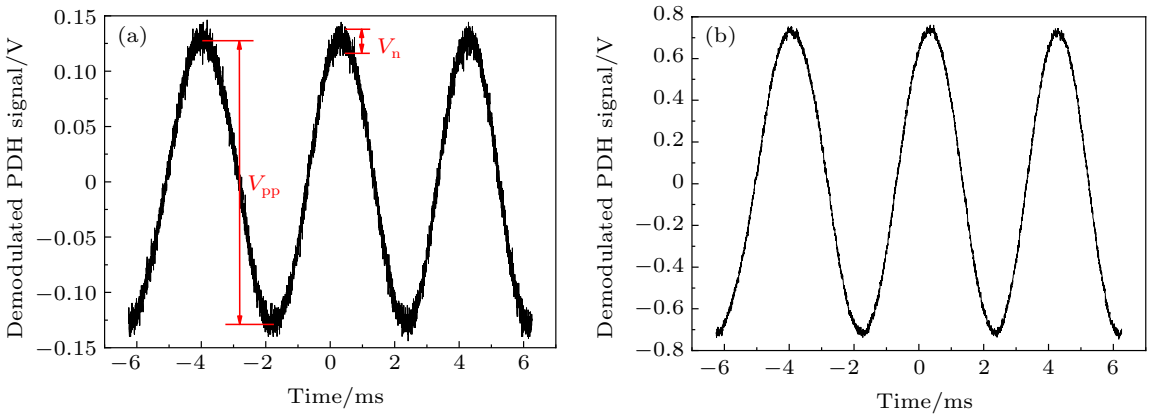

Fig. 4. Error signals from (a) existing RPD and (b) new-designed RPD. The weak beam is −40 dBm for both cases. The power of the local beam is 0 dBm.

to the noise of the curve (V_n in Fig. 4). The power of the local beam remains unchanged, the power of the signal beam increases from −70 dBm to −20 dBm with a step of 5 dBm. The measured SNRs are shown in Fig. 5. As the power of the signal beam increases, the SNRs with the existing and new-designed RPDs also increase linearly. Under the same conditions, the SNR with the new-designed RPD is about 15 dB higher than that with the existing RPD. Utilizing the new-designed RPD, we can achieve a stable phase locking when the signal power is only −70 dBm.

The performances of the existing and new-designed RPDs are experimentally demonstrated by comparing the standard deviations of the stability curves. Figure 6(a) is the measured

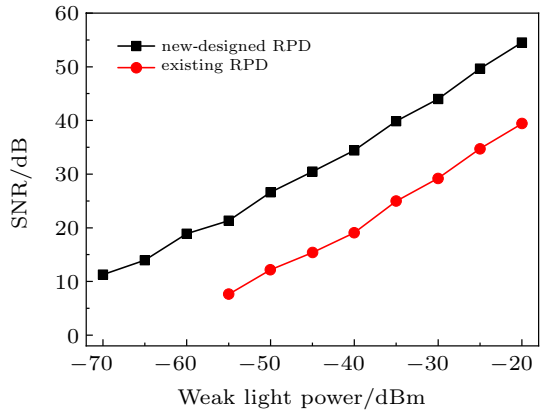

Fig. 5. The SNRs of existing and new-designed RPDs at different power of weak beam when the power of the local beam is 0 dBm.

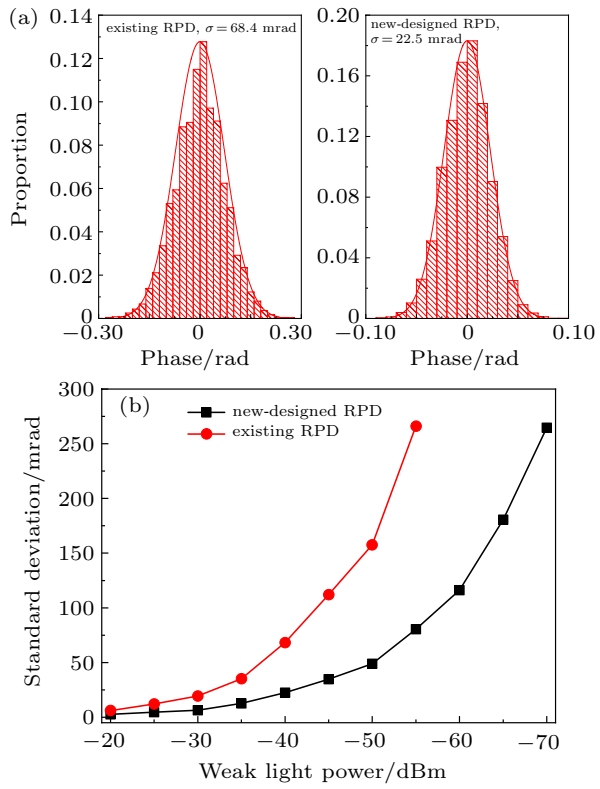

Fig. 6. Comparison of standard deviations of the stability curves. (a) Standard deviations with the existing and new-designed RPDs at the signal power of −40 dBm. (b) Standard deviations at different power of signal beam when the local power is 0 dBm.

results at the signal power of −40 dBm. By fitting the relative frequency distributions of the error signals with a Gaussian function,[31,32] the standard deviations with the existing and new-designed RPDs are 68.4 mrad and 22.5 mrad, respectively. The standard deviations are compared at different signal beam power from −20 dBm to −70 dBm, with a step of 5 dBm, which are shown in Fig. 6(b). As the signal power is decreased, the standard deviations increase exponentially. When the signal power is less than −55 dBm, the error signal from the existing RPD is completely merged in noise. Instead the feedback loop operates stably with a standard deviation of 80.52 mrad with the new-designed RPD. The results indicate that the new-designed RPD can effectively improve the performance of quantum optics experiments.[28,29] Utilizing the sub-nW locking technique, we have experimentally completed the demonstration of channel multiplexing quantum communication.[33]

4. Conclusion and perspectives

We present a RPD with Q factor of 320.83 at the resonant frequency of 38.5 MHz on the basis of a theoretical analysis. With new-designed RPD, we measure the SNRs of the error signals and the standard deviations of the stability curves. Under the same conditions, the SNR with the new-designed RPD is about 15 dB higher than that with the existing RPD. For the signal beam of −40 dBm, the standard deviations with the existing and new-designed RPDs are 68.4 mrad and 22.5 mrad, respectively. Due to the dramatic improvement of ultralow power extraction, the new-designed RPD has helped us to complete the demonstration of channel multiplexing quantum communication.[33]

References

[1] Hou L, Han H N, Wang W, Zhang L, Pang L H, Li D H and Wei Z Y 2015 *Chin. Phys. B* **24** 024213
[2] Salomon C, Hils D and Hall J L 1988 *J. Opt. Soc. Am. B.* **5** 1576
[3] Fescenko I, Alnis J, Schliesser A, Wang C Y, Kippenberg T J and Hänsch T W 2012 *Opt. Express* **20** 19185
[4] Jin X J, Lin Y, Lu Y, Ma H L and Jin Z H 2018 *Appl. Opt.* **57** 5789
[5] Wang J Q and He L X 2018 *Acta. Sin. Quantum. Opt.* **24** 371 (in Chinese)
[6] Yu J, Qin Y, Yan Z H, Lu H D and Jia X J 2019 *Opt. Express* **27** 3247
[7] Abramovici A, Althouse W E, Drever R W P, Gursel Y, Kawamura S J, Raab F J, Shoemaker D, Sievers L, Spero R E, Thorne K S, Vogt R E, Weiss R, Whitcomb S E and Zucker M E 1992 *Science* **256** 325
[8] Liu H, Gao F, Wang Y B, Tian X, Ren J, Lu B Q, Xu Q F, Xie Y L and Chang H 2015 *Chin. Phys. B* **24** 013201
[9] Chow J H, McClelland D E, Gray M B and Littler I C M 2005 *Opt. Lett.* **30** 1923
[10] Wang H M, Xu Z S, Ma S C, Cai M H, You S H and Liu H P 2019 *Opt. Lett.* **44** 5816
[11] Hao L P, Xue Y M, Fan J B, Bai J X, Jiao Y C and Zhao J M 2020 *Chin. Phys. B* **29** 033201
[12] Young B C, Cruz F C, Itano W M and Bergquist J C 1999 *Phys. Rev. Lett.* **82** 3799
[13] Shen D N, Ding L Y, Zhang Q X, Zhu C H, Wang Y X, Zhang W and Zhang X 2020 *Chin. Phys. B* **29** 074210
[14] Spencer D T, Davenport M L, Komljenovic T, Srinivasan S and Bowers J E 2016 *Opt. Express* **24** 13511

[15] Dai D P, Xia Y, Yin Y N, Yang X X, Fang Y F, Li X J and Yin J P 2014 *Opt. Express* **22** 28645
[16] He Q X, Zheng C, Lou M H, Ye W L, Wang Y D and Tittel F K 2018 *Opt. Express* **26** 15436
[17] Rafael J, Abdel-Baset M A I, Pankaj K C and Hichem E 2018 *Chin. Phys. B* **27** 114206
[18] Xiang S H, Zhu X X and Song K h 2018 *Chin. Phys. B* **27** 100305
[19] Takeno Y, Yukawa M, Yonezawa H and Furusawa A 2007 *Opt. Express* **15** 4321
[20] Liu Q, Feng J X, Li H, Jiao Y C and Zhang K S 2012 *Chin. Phys. B* **21** 104204
[21] Feng Y Y, Shi R H and Guo Y 2018 *Chin. Phys. B* **27** 020302
[22] Yang W H, Shi S P, Wang Y J, Ma W G, Zheng Y H and Peng K C 2017 *Opt. Lett.* **42** 4553
[23] Sun X C, Wang Y J, Tian L, Zheng Y H and Peng K C 2019 *Chin. Opt. Lett.* **17** 072701
[24] The LIGO Scientific Collaboration 2013 *Nat. Photon.* **7** 613
[25] Dooley K L, Schreiber E, Vahlbruch H, Affeldt C, Leong J R, Wittel H and Grote H 2015 *Opt. Express* **23** 8235
[26] Oelker E, Mansell G, Tse M, Miller J, Matichard F, Barsotti L, Fritschel P, McClelland D E, Evans M and Mavalvala N 2016 *Optica* **3** 682
[27] Black E D 2001 *Am. J. Phys* **69** 79
[28] Chen C Y, Li Z X, Jin X L and Zheng Y H 2017 *Rev. Sci. Instrum.* **88** 099901
[29] Chen C Y, Shi S P and Zheng Y H 2017 *Rev. Sci. Instrum.* **88** 103101
[30] Serikawa T and Furusawa A 2018 *Rev. Sci. Instrum.* **89** 063120
[31] Jia M Y, Zhao G, Zhou Y T, Liu J X, Guo S J, Wu Y Q, Ma W G, Zhang L, Dong L, Yin W B, Xiao L T and Jia S T 2018 *Acta. Phys. Sin.* **67** 104207 (in Chinese)
[32] Zhao G, Hausmaninger T, Ma W G and Axner O 2017 *Opt. Lett.* **42** 3109
[33] Shi S P, Tian L, Wang Y J, Zheng Y H, Xie C D and Peng K C 2020 *Phys. Rev. Lett.* **125** 070502